Quantitative comparison of real and CEMHYD3D model microstructures using correlation functions

by

Dale P. Bentz
Building and Fire Research Laboratory
National Institute of Standards and Technology
Gaithersburg, MD 20899 USA

Reprinted from Cement and Concrete Research, Vol. 36, No .2, pp. 259-263, 2006.

National Institute of Standards and Technology
Technology Administration, U.S. Department of Commerce

Available online at www.sciencedirect.com

SCIENCE DIRECT®

Cement and Concrete Research 36 (2006) 259 – 263

Cement and Concrete Research

Quantitative comparison of real and CEMHYD3D model microstructures using correlation functions

Dale P. Bentz *

Materials and Construction Research Division, National Institute of Standards and Technology 100 Bureau Drive Stop 8615, Gaithersburg, MD 20899-8615 USA

Received 25 September 2004; accepted 26 July 2005

Abstract

A quantitative comparison of real and computer-generated (model) cement paste microstructures based on the analysis of three-dimensional image sets is presented. In addition to a visual presentation of extracted two-dimensional images, the comparison is based on the calculation of the normalized two-point correlation function for a variety of phases including unhydrated cement, hydration products, and capillary porosity. A favorable comparison is observed between model and real microstructures for both the two-dimensional images and the computed correlation functions. Several interesting observations from the correlation analysis are introduced and discussed. This analysis provides one further validation of the use of microstructure models to predict the microstructure and properties of cement-based materials.

Keywords: Image analysis; Microstructure; Modeling; X-ray tomography

1. Introduction

In recent years, a paradigm shift from manual to virtual testing of cement and concrete has nucleated [1]. While perhaps still in its induction stage, numerous examples of the ability of microstructure models to predict a wide variety of the performance properties of cement-based materials have been presented [2–5]. Despite their success in predicting properties, the creditability of these models is still questioned by some. To accelerate their acceptance, a direct comparison of model and real microstructures would be beneficial.

While comparisons between two-dimensional images of real and model microstructures were presented in one of the first two papers [6] describing the CEMHYD3D microstructure model, a direct three-dimensional comparison was not possible at that time. However, with the development of the Visible Cement Data Set [7] (currently available at http://visiblecement.nist.gov), a direct comparison between real and computer model three-dimensional microstructures is now possible. The Visible Cement Data Set consists of a series of X-ray computed microtomographic 3-D images of unhydrated and hydrated cement pastes (along with a few images of hydrating calcium sulfate hemihydrate) obtained with a voxel dimension of 0.95 μm at the European Synchrotron Radiation Facility (ESRF) in 2000. The data were acquired for Cement and Concrete Reference Laboratory (CCRL) proficiency cement sample 133 [8], which has been used extensively in the development and refinement of the CEMHYD3D microstructure model [9]. In this paper, a direct and quantitative comparison between the X-ray microtomography images and images generated by the CEMHYD3D microstructure model is presented.

2. Procedures

For the comparison, the X-ray microtomography images of CCRL cement 133 mixed at a nominal water-

* Tel.: +1 301 975 5865; fax: +1 301 990 6891.
E-mail address: dale.bentz@nist.gov.

0008-8846/$ - see front matter © 2005 Elsevier Ltd. All rights reserved.
doi:10.1016/j.cemconres.2005.07.003

to-cement ratio (w/c) of 0.45 were selected [7]. An image set obtained 3 h after mixing was used as being representative of the starting microstructure prior to any hydration. An image set obtained after 137 h of hydration (at about 25 °C) was selected to represent a well-hydrated microstructure. $300 \times 300 \times 300$ voxel subvolumes were extracted from each tomographic image to use for further characterization and analysis. As stated previously, the images were obtained with a voxel dimension of 0.95 μm. Individual phases (porosity, cement particles, and hydration products) were segmented from the raw data image based on analysis of the image's greylevel histogram, as described previously [7]. The segmented three-dimensional images were then input into the correlation analysis programs.

Simulations were conducted using the latest version of the CEMHYD3D microstructure model being developed in the ongoing Virtual Cement and Concrete Testing Laboratory (VCCTL) consortium. The spatial resolution was set at 1 μm/pixel and simulations of both $100 \times 100 \times 100$ and $200 \times 200 \times 200$ microstructures were completed. The measured particle size distribution for cement 133 [10] was used to create a starting three-dimensional model microstructure of cement (and gypsum) particles in water. It should be clarified that the 3 h microtomography image was *not* used as a direct input to the CEMHYD3D hydration model, but rather only to extract individual 3-D particle shapes [11]. Either digitized spheres or these real-shaped particles were then used to fill a three-dimensional cubic volume to the prescribed w/c ratio, utilizing periodic boundary conditions at the cube faces and edges. The hydration models were executed to match both the measured w/c and degree of hydration of the real system, 0.47 and 0.62, respectively [7]. In accordance with the experimental conditions [7], hydration was conducted under sealed (and isothermal) conditions. Initial and final (post hydration) microstructures were analyzed using the same correlation analysis as that performed on the segmented real microstructure images. No segmentation per se was required for the model images, as the CEMHYD3D software outputs an image in which each voxel is already uniquely identified as a single phase.

Two-point correlation functions were computed for single or multiple phases using the following equation for an M × N image:

$$S(x,y) = \sum_{i=1}^{M-x} \sum_{j=1}^{N-y} \frac{I(i,j)I(x+i,y+j)}{(M-x)(N-y)} \quad (1)$$

where $I(i,j)=1$ if the voxel at location (i,j) contains the phase(s) of interest and $I(i,j)=0$ otherwise. $S(x,y)$ was computed over all (100, 200, or 300) of the two-dimensional slices through the thickness of the three-dimensional microstructures. Since there is no inherent anisotropy in either the real or simulated microstructures, a complete three-dimensional correlation analysis was deemed unnecessary. These values were then converted to $S(r)$ for distances r in voxels (or micrometers) by [12]:

$$S(r) = \frac{1}{2r+1} \sum_{l=0}^{2r} S\left(r, \frac{\pi l}{4r}\right). \quad (2)$$

Finally, the normalized two-point correlation function was calculated as:

$$N(r) = \frac{(S(r) - S(0)*S(0))}{(S(0) - S(0)*S(0))}. \quad (3)$$

Results are presented in terms of the normalized correlation functions to eliminate the minor influence of variable volumetric phase fractions between the model and real microstructure images. It is worth noting that $S(0)$ simply represents the volume fraction of the phase(s) of interest in the three-dimensional microstructure and $N(0)=1$. For large values of r, the probability of two voxels having the same phase(s) is simply a random process, with $S(r)$ approaching a value of the volume fraction of the phase(s) of interest squared. In this case, $N(r)$ approaches a value of 0. The initial slope of the $S(r)$ function is proportional to the specific surface of the phase(s) of interest. More information on spatial correlation functions and their usage to predict physical proper-

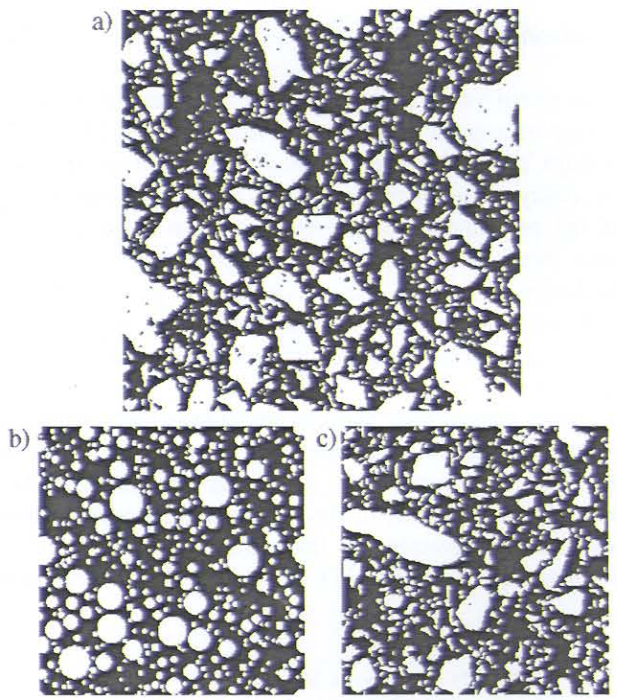

Fig. 1. Initial 2-D images from experimental and model systems: (a) real system (285 by 285 μm), (b) model system with spherical particles, and (c) model system with real particle shapes (200 by 200 μm).

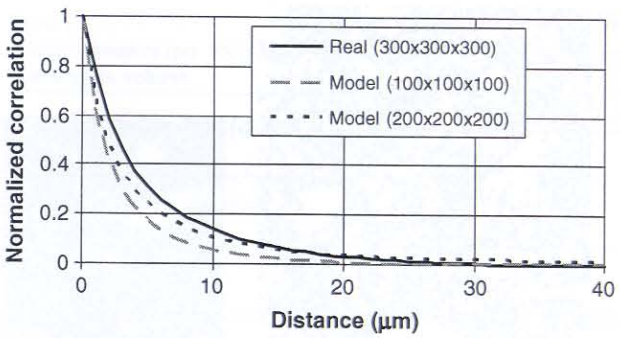

Fig. 2. Measured normalized correlation functions for initial real and model microstructures showing the influence of model system size.

ties such as permeability can be found in Ref. [12] and [13].

3. Results and discussion

Fig. 1 presents two-dimensional images from the initial starting microstructures for the real cement paste and for two model cement pastes generated with spherical and real particle shapes, respectively. Initially, attempts were made to model the cement paste using a $100 \times 100 \times 100$ microstructure model. However, this resulted in a system with too fine of cement particles (as indicated by the more rapid decay of the normalized correlation function in Fig. 2), relative to the real $300 \times 300 \times 300$ microstructure. Increasing the system size to 200^3 allowed for a truer representation of the "larger" cement particles (maximum diameter = 65 μm) present in the starting cement 133 microstructure, and resulted in a correlation function that basically overlaps the one measured on the real starting microstructure. As shown in Fig. 3, the correlation functions for the 200^3 microstructures based on spherical and real-shaped particles both basically overlap that obtained for the real system.

Next, the microstructures following hydration are considered. Fig. 4 shows the two-dimensional images for the unhydrated cement particles in the real and model microstructures, while their normalized correlation functions are provided in Fig. 5. Similar features are observed in the two-dimensional images and the correlation functions basically overlap one another for distances beyond 10 μm. There is an indication that the particles in the model system are "rougher" in both the visual image and in the higher initial slope of the correlation function in Fig. 5. This is most likely due to the pixel-based nature and inherent finite resolution of the CEMHYD3D model where individual voxels dissolve, diffuse, and react within the available pore space [2]. In Fig. 5, no substantial difference is observed between the normalized correlation functions for the two model systems based on spherical and real particle shapes. This observation also holds true for the results to be subsequently presented for the hydration products and capillary pores, indicating that the use of spherical as opposed to real-shaped particles appears to have a negligible influence on the resultant microstructures in the CEMHYD3D model for a degree of hydration of 0.62. Thus, it seems to be much more important to adequately capture the particle size distribution of the particles (Fig. 2) than their specific shapes. In this regard, it is worth noting that spherical particles are typically assumed in the derivation of a particle size distribution from either experimental light scattering or sieve measurements.

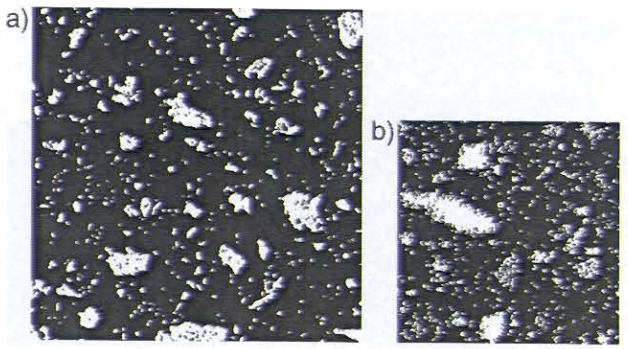

Fig. 4. 2-D images from experimental and model hydrated systems showing remaining unhydrated cement particles: (a) real system, (b) model system with real particle shapes.

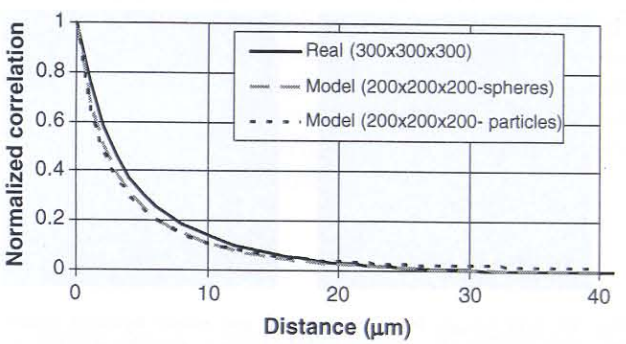

Fig. 3. Measured normalized correlation functions for initial real and model microstructures showing the influence of model particle shape.

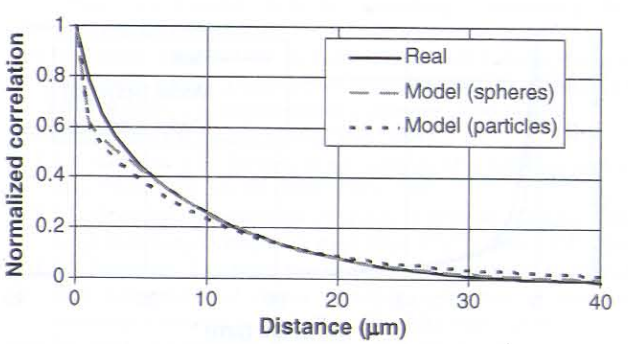

Fig. 5. Measured normalized correlation functions for hydrated real and model microstructures for the remaining cement particles.

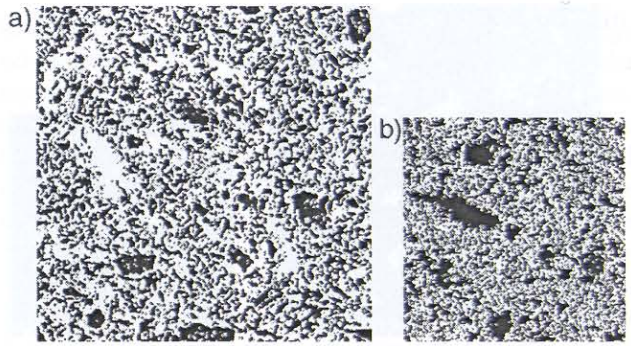

Fig. 6. 2-D images from experimental and model hydrated systems showing hydration products: (a) real system, (b) model system with real particle shapes.

Surprisingly, the correlation distance, defined as how long it takes the normalized correlation function to decay to a value near 0, is actually larger in all three of the hydrated microstructures (Fig. 5) than in the initial microstructures (Fig. 3). The physical explanation of this seemingly perplexing behavior is that many of the smaller cement particles have completely hydrated by this point, so that the unhydrated particle correlation functions in the hydrated systems are dominated by the remaining "larger" cement particles.

The two-dimensional images and normalized correlation functions for all of the hydration products are presented in Figs. 6 and 7, respectively. Once again, reasonable agreement is observed between the real and model microstructures. The corresponding figures for the capillary porosity phase are provided in Figs. 8 and 9. Observing the normalized correlation functions in Fig. 9, there is an indication that the capillary porosity in the model system is slightly finer than that in the real microstructure. This porosity would be even finer if the model were executed under saturated as opposed to sealed conditions. As indicated by the grey (empty) pores in the model system in Fig. 8, a substantial contribution to the "coarse" porosity in the hydrated microstructure is the presence of these large pores that are the first to empty under sealed curing conditions, due to self-desiccation. This observation points out the importance of proper curing of higher w/c

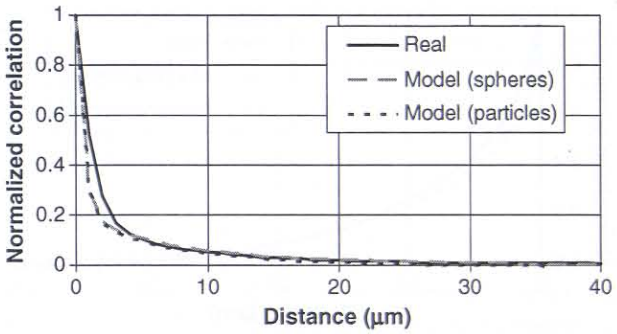

Fig. 7. Measured normalized correlation functions for hydrated real and model microstructures for all of the hydration products.

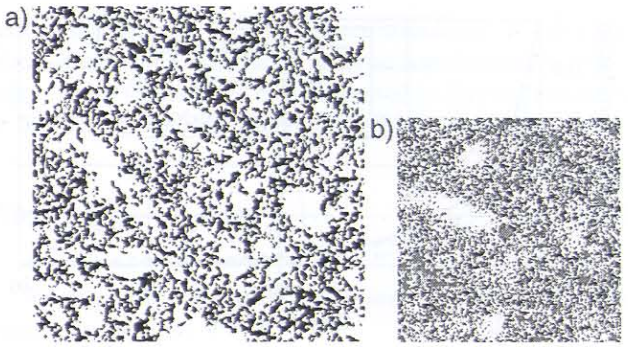

Fig. 8. 2-D images from experimental and model hydrated systems showing capillary porosity (in black): (a) real system, (b) model system (empty pores in grey).

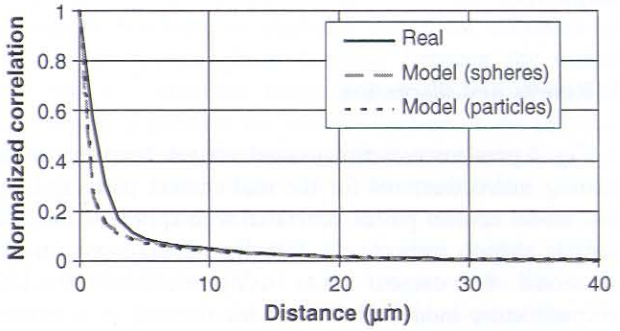

Fig. 9. Measured normalized correlation functions for hydrated real and model microstructures for the capillary porosity (water-filled and empty).

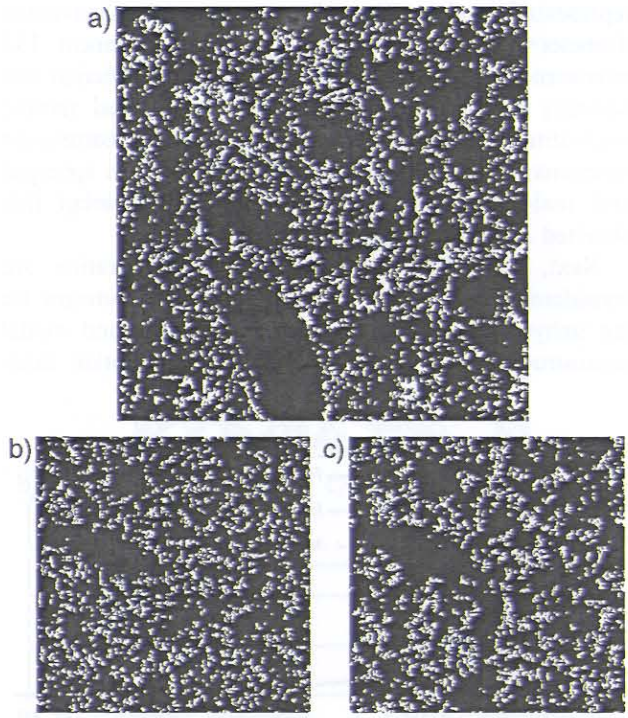

Fig. 10. 2-D images from experimental and model hydrated systems showing calcium hydroxide (in white): (a) real system, (b) model system with a high nucleation probability for CH, and (c) model system with a 100× lower nucleation probability for CH.

Table 1
Number densities (per 100 × 100 × 100 μm volume) of CH particles larger than a given volume

	>65 μm^3	>100 μm^3	>1000 μm^3
Real	104.3	63.3	8.6
Model (high nucleation probability)	396	243	0.375
Model (100× lower nucleation probability)	118	97.6	25.4

concretes, as well as lower w/c ones, to avoid the formation of large empty pores that may remain throughout the lifetime of the material. A further analysis was performed on the connectivity or percolation of the capillary porosity in the real and model microstructures using a computational burning algorithm [14]. Percolated porosity fractions of 98% [7] and 85% were measured for the real and model systems, respectively, indicating a slightly more connected pore structure for the real system.

While it is difficult to distinguish individual hydration product phases in the real microstructure, attempts were made to isolate the calcium hydroxide (CH) phase for a visual comparison. The greylevel histogram for the real microstructure was analyzed and a threshold selected to give a CH volume fraction that matched that expected for the measured amount of hydration (about 12% CH by volume), after the "false" CH rims around each hydrating cement particle were removed by a simple 3-D erosion algorithm. Fig. 10a provides a two-dimensional image of the "segmented" CH particles. Model representations of the CH distribution are provided in Fig. 10b and c for two choices for the parameter that controls the nucleation of CH crystals within the CEMHYD3D microstructure model [2,9]. For a more quantitative analysis, the CH particle densities were measured in each 3-D microstructure as the number of separate CH "particles" larger than a given volume, using a particle burning algorithm with 6-neighbor (voxel) connectivity. Thus, two CH voxels connected by a voxel face were considered to be part of the same particle, while two voxels connected only at an edge or a corner point were counted as individual particles. The results for three values of the minimum particle volume are provided in Table 1. From the table, clearly the 100× lower value for the CH nucleation probability provides a distribution of (large) CH particle sizes that is in better overall agreement with that measured on the real hydrated microstructure. Additionally, this lower value for CH nucleation gives the better visual agreement with the real microstructure image in Fig. 10, as the human eye and brain are also likely biased by the larger particles present in a two-dimensional black and white image.

4. Conclusions

Based on a visual comparison of extracted two-dimensional images and a numerical comparison of normalized correlation functions, good agreement between the three-dimensional microstructure of real and CEMHYD3D hydrated cement pastes has been observed. The analysis has also provided insights into the increasing correlation distance observed for the unhydrated cement particles, the strong influence of sealed curing on the maintenance of a set of coarse pores in the hydrating microstructure, and the proper selection of parameters controlling the nucleation of calcium hydroxide crystals within the simulated microstructures.

Acknowledgements

The author would like to thank Dr. Daniel Quenard of the Centre Scientifique et Technique du Batiment (Grenoble, France) for introducing him to the application of correlation functions to images, now many years ago.

References

[1] D.P. Bentz, E.J. Garboczi, J.W. Bullard, C.F. Ferraris, N.S. Martys, P.E. Stutzman, Virtual testing of cement and concrete, ASTM STP 169D Significance of Tests and Properties of Concrete and Concrete-making Materials, 2005.
[2] D.P. Bentz, Three-dimensional computer simulation of portland cement hydration and microstructure development, J. Am. Ceram. Soc. 80 (1) (1997) 3–21.
[3] D.P. Bentz, E.J. Garboczi, C.J. Haecker, O.M. Jensen, Effects of cement particle size distribution on performance properties of cement-based materials, Cem. Concr. Res. 29 (1999) 1663–1671.
[4] C.J. Haecker, D.P. Bentz, X.P. Feng, P.E. Stutzman, Prediction of cement physical properties by virtual testing, Cem. Int. 1 (3) (2003) 86–92.
[5] A. Princigallo, P. Lura, K. van Breugel, G. Levita, Early development of properties in a cement paste: a numerical and experimental study, Cem. Concr. Res. 33 (2003) 1013–1020.
[6] D.P. Bentz, E.J. Garboczi, A digitized simulation model for microstructural development, Advances in Cementitious Materials, Ceramics Transactions, vol. 16, 1991, pp. 211–226.
[7] D.P. Bentz, S. Mizell, S. Satterfield, J. Devaney, W. George, P. Ketcham, J. Graham, J. Porterfield, D. Quenard, F. Vallee, H. Sallee, E. Boller, J. Baruchel, The visible cement data set, J. Res. Natl. Inst. Stand. Technol. 107 (2) (2002) 137–148.
[8] Cement and Concrete Reference Laboratory, Cement and Concrete Reference Laboratory Proficiency Sample Program: Final Report on Portland Cement Proficiency Samples Number 133 and 134, Cement and Concrete Reference Laboratory, Gaithersburg, MD, 1999 (September).
[9] D.P. Bentz, CEMHYD3D: A Three-Dimensional Cement Hydration and Microstructure Development Modelling Package. Version 2.0, NISTIR 6485, U.S. Department of Commerce, 2000 (April).
[10] vcctl.cbt.nist.gov (access verified June 2005).
[11] E.J. Garboczi, J.W. Bullard, Shape analysis of a reference cement, Cem. Concr. Res. 34 (10) (2004) 1933–1937.
[12] J.G. Berryman, Measurement of spatial correlation functions using image processing techniques, J. Appl. Phys. 57 (7) (1985) 2374–2384.
[13] J.G. Berryman, S.C. Blair, Use of digital image analysis to estimate fluid permeability of porous materials: application of two-point correlation functions, J. Appl. Phys. 60 (1986) 1930–1938.
[14] D.P. Bentz, E.J. Garboczi, Percolation of phases in a three-dimensional cement paste microstructure model, Cem. Concr. Res. 21 (2) (1991) 325–344.